Turbulent transport characteristics of coherent structures in ideal urban morphology based on wind tunnel experiments

Guoliang Chen[1*], Chun-Ho Liu[1], Ziwei Mo[2]
[1] Department of Mechanical Engineering, The University of Hong Kong, 7/F, Haking Wong Building Pokfulam Road, Hong Kong, China
[2] School of Atmospheric Sciences, Sun Yat-sen University, & Southern Marine Science and Engineering Guangdong Laboratory (Zhuhai), Zhuhai, China
* Corresponding author.
*E-mail addresses: glchen97@connect.hku.hk (G. Chen)

ABSTRACT:

Considering the impact of individual roughness elements, turbulence within urban roughness sublayers (RSLs) is characterized by its non-uniformity. This paper employs the phase-space algorithm to uncover coherent structures, serving as a solution approach to investigate the transport mechanism across urban morphology. The drag coefficient *Cd*, a measure of surface roughness, is utilized to examine the influence of (idealized) urban morphology on canopy-level dynamics and ventilation. Wind tunnel experiments are conducted to study the flows and turbulence within urban canopy layers (UCLs) under various aerodynamic roughness conditions.
Keywords: Drag coefficient C_d, Phase-space algorithm, Wind tunnel experiment

1. Introduction

In rapidly developing cities, the air quality has emerged as a significant public concern, particularly when compared to rural areas, due to the high population density (Lawal et al., 2023; Vidanapathirana et al., 2023). The extensive construction and bulky architectural layout in urban areas inevitably hinder the efficient removal of stale air from, or the entry of fresh air into, urban canopy layers (UCLs). As a result, this degradation severely impacts the air quality at street level (Edward, 2009; Leung et al., 2012; Zhang et al., 2022; Liang et al., 2023). Hence, it is crucial to develop an advanced understanding of the dynamics within the atmospheric surface layers (ASLs) over buildings. This understanding is essential for enhancing street-level ventilation and improving air quality (Oke, 1988; Jiménez, 2004; Michioka et al., 2023).

Coherent structures can be detected with the assistance of a range of detection algorithms. Coherent-structure detections, such as U-level (Bogardt and Tiederman, 1986), window average gradient (WAG) (Antonia and Bisset, 1990; Krogstad et al., 1998), variable interval time average (VITA) (Bogardt and Tiederman, 1986), temporal average (TPAV) (Wallace et al., 1977), quadrant (Lu and Willmarth, 1973; Wallace, 2016), and phase-space filtering (Goring and Nikora, 2002), are commonly adopted. Recently, there have been advancements in the conventional phase-space filtering (Goring and Nikora, 2002) by incorporating central differencing (Wu et al., 2005) to analyze 3D physical quantities such as velocity fluctuation, acceleration, and jerk. This approach provides a more comprehensive perspective for studying and understanding the dynamics of turbulent flows.

Building upon the phase-space algorithm proposed by Wu et al. (2022) and conducting wind tunnel experiments with various configurations of roughness elements, this study aims to explore the coherent structures within turbulent flows. Specifically, the focus is on understanding the characteristics of these structures and their role in contributing to the momentum flux over an idealized urban morphology.

2. Wind tunnel experiments

The experiments were performed in an isothermal, open-circuit wind tunnel located at the Department of Mechanical Engineering, The University of Hong Kong, as illustrated in Fig. 1. The test section of the wind tunnel is constructed using acrylic and has dimensions of 6 meters in length, 0.56 meters in width, and 0.56 meters in height. To simulate idealized urban areas, roughness elements were affixed to the entire 6-meter floor of the wind tunnel, facilitating the generation of fully developed turbulent-boundary-layer (TBL)

DOI 10.5258/WES/P0002

flows. Each measurement point had a sampling duration of over 40 seconds, and the sampling frequency was set at 2 kHz.

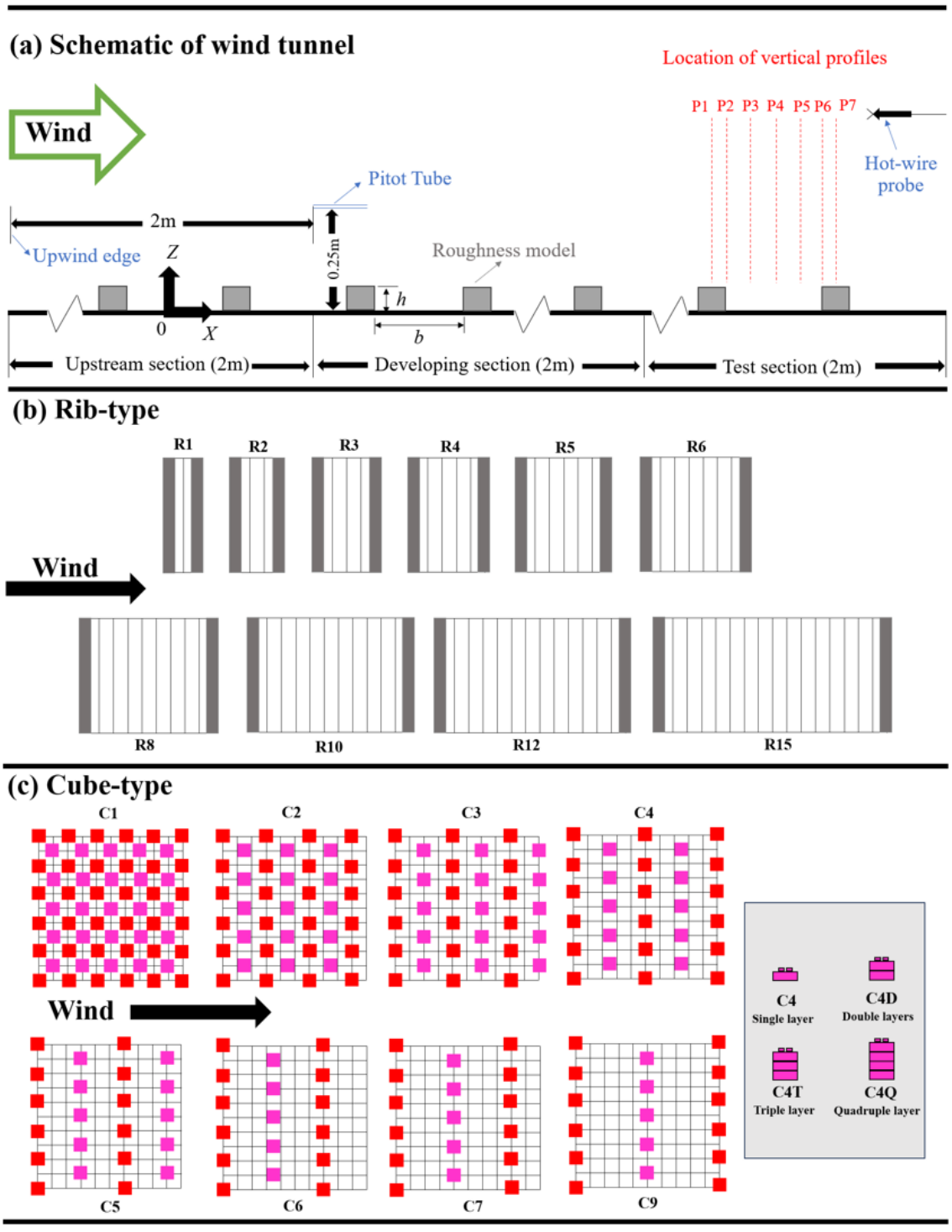

Fig. 1. Configurations of roughness elements employed in the wind tunnel experiments.

3. Results and discussion

When analyzing the data, it was observed that the number of detected coherent-structure data points initially encompassed all data points when k = 0. However, as the

DOI 10.5258/WES/P0002

value of k increased, the number of coherent-structure data points gradually decreased until it reached zero when k = 1 (as shown in **Fig. 2a**). Additionally, the count of discrete turbulent events (defined as consecutive coherent data points) followed a distinct pattern. It started with one event at k = 0, peaked at around k = 0.25, and then decreased to zero when k = 1 (**Fig. 2b**). It is worth noting that in **Fig. 2b**, all data points were contained within the ellipsoid, indicating that no turbulent events were detected.

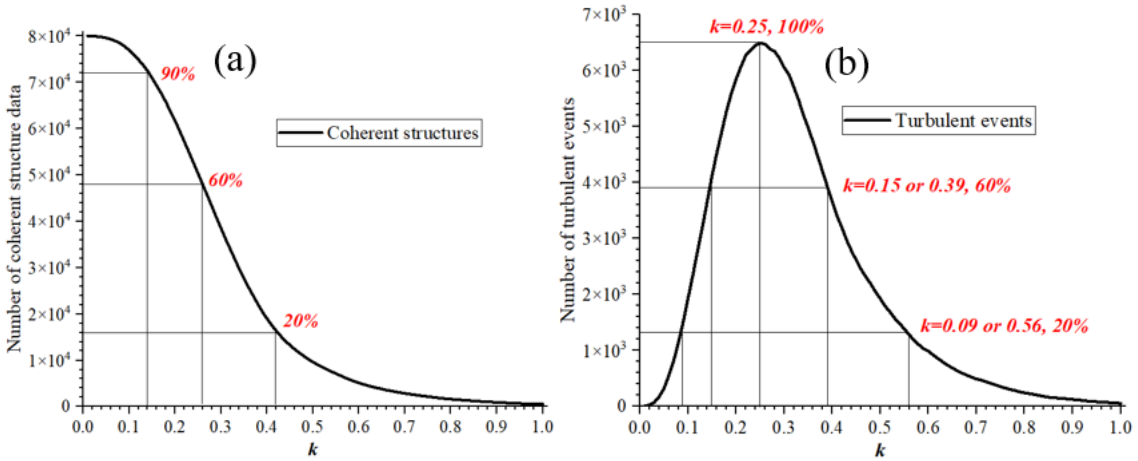

Fig. 2. Coherent-structure data points and the associated turbulent events. Number of detected: (a) coherent structure data points and (b) discrete turbulent events versus the scaling factor k. Measurement location P1 at z = h in R4 case is taken as an example.

Fig. 3 illustrates the relationship between exuberance (η), drag coefficient (Cd), and the scaling factor (k). In the high-drag-coefficient regime (with Cd values ranging from 4.1×10^{-3} to 10.8×10^{-3} in rib-type arrays), the exuberance η is relatively unaffected by changes in the drag coefficient Cd, except for a slight increase (peaking at approximately -0.33 to -0.3) observed between cases R1 and R2. This increase corresponds to a variation of approximately 9% (as shown in **Fig. 3a**). Conversely, in the low-drag-coefficient regime (with Cd values ranging from 3.6×10-3 to 7.9×10-3) in cube-type arrays, the exuberance η is significantly influenced by the drag coefficient Cd. The peaked exuberance values fall within the range of -0.41 to -0.21, representing a substantial change of around 50% (as depicted in **Fig. 3b**).

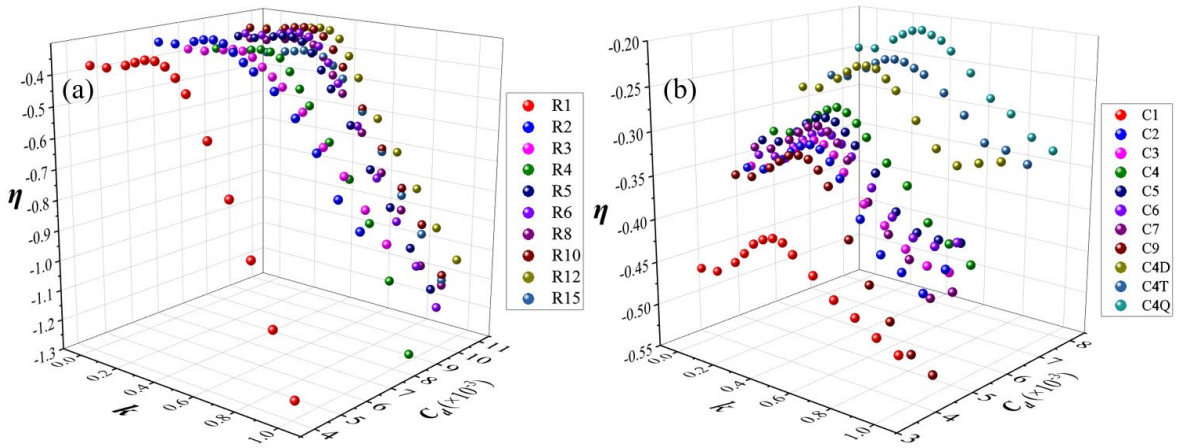

Fig. 3. Correlation among exuberance η, drag coefficient Cd, and scaling factor k for (a) rib-type arrays and (b) cube-type arrays at z = h.

DOI 10.5258/WES/P0002

4. Conclusion

In this study, wind tunnel measurements were conducted on two different idealized urban morphologies. The focus of the research was to investigate the coherent structures detected using the phase-space algorithm and to elucidate the ventilation mechanism of urban canyons. The research findings can serve as valuable references for urban planning and architectural layout. For instance, they suggest that appropriate adjustments, such as increasing building spacing, adjusting building height, and changing building arrangement from aligned to staggered, can significantly improve air transport efficiency. Furthermore, promoting the influence of high-frequency and small-scale motion in turbulence on air circulation can help enhance the air quality within the urban canopy. By implementing these measures, cities can work towards improving air quality and achieving sustainable urban development goals.

REFERENCES

[1] Lawal, O., Ogugbue, C. J., & Imam, T. S. (2023). Mining association rules between lichens and air quality to support urban air quality monitoring in Nigeria. *Heliyon, 9*, e13073.

[2] Vidanapathirana, M., Perera, N., Emmanuel, R., & Coorey, S. (2023). Air pollutant dispersion around high-rise building cluster forms: The case of Port City, Colombo, Sri Lank. *In Environmental Science and Pollution Research, 30*, 94166–94184.

[3] E. Ng. (2009). Policies and technical guidelines for urban planning of high-density cities–air ventilation assessment (AVA) of Hong Kong, *Building and Environment, 44*, 1478–1488.

[4] Leung, K. K., Liu, C. H., Wong, C. C. C., Lo, J. C. Y., & Ng, G. C. T. (2012). On the study of ventilation and pollutant removal over idealized two-dimensional urban street canyons. *Building Simulation, 5*, 359–369.

[5] Zhang, A., Xia, C., & Li, W. (2022). Exploring the effects of 3D urban form on urban air quality: Evidence from fifteen megacities in China. *Sustainable Cities and Society, 78*, Article 103649.

[6] Liang, M., Chao, Y., Tu, Y., & Xu, T. (2023). Vehicle pollutant dispersion in the urban atmospheric environment: A review of mechanism, modeling, and application. *Atmosphere, 14*, 279.

[7] T.R. Oke. (1988). Street design and urban canopy layer climate, *Energy and Buildings, 11*, 103–113.

[8] J. Jiménez. (2004). Turbulent flows over rough walls, *Annual Review of Fluid Mechanics*. 36, 173–196.

[9] Michioka, T., Funaki, R., & Kawai, T. (2023). Effects of building arrays on large-scale turbulent motions within an urban canopy. *Boundary-Layer Meteorology*.

[10] Bogardt, D. G., & Tiederman, W. G. (1986). Burst detection with single-point velocity measurements. *Journal of Fluid Mechanics, 162*, 389–413.

[11] Krogstad, P.-A., Kaspersen, J. H., & Rimestad, S. (1998). Convection velocities in turbulent boundary layers. *Physics of Fluids, 10*,949.

[12] Wallace, J. M., Brodkey, R. S., & Eckelmann, H. (1977). Pattern-recognized structures in bounded turbulent shear flows. *Journal of Fluid Mechanics, 83(4)*, 673–693.

[13] Lu, S. S., & Willmarth, W. W. (1973). Measurements of the structure of the Reynolds stress in a turbulent boundary layer. *Journal of Fluid Mechanics, 60(3)*, 481–511.

[14] Goring, D. G., & Nikora, V. I. (2002). Despiking acoustic doppler velocimeter data. *Journal of Hydraulic Engineering,128(1)*, 117–126.

[15] Wu, B., Bao, H., Ou, J., & Tian, S. (2005). Stability and accuracy analysis of the central difference method for real-time substructure testing. *Earthquake Engineering and Structural Dynamics*, 34(7), 705–718.

[16] Wu, J., Krynkin, A., & Croft, M. (2022) Objective phase-space identification of coherent turbulent structures in 1D time series. *Journal of Hydraulic Research, 60*, 811–825.

DOI 10.5258/WES/P0002